Received: 14 June 2025 | Accepted: 24 November 2025

DOI: 10.1111/eci.70162

ORIGINAL ARTICLE

WILEY

Fibroblast-driven MMP-9/TIMP-1 imbalance in bronchoalveolar lavage reflects fibrotic progression in interstitial lung disease

Maria Bertolotto[1,2] | **Daniela de Totero**[3] | **Paolo Giannoni**[4] | **Emanuela Barisione**[5] | **Marco Grosso**[5] | **Ennio Nano**[3] | **Roberto Fiocca**[6,7] | **Simona Pigozzi**[6,7] | **Elisabetta Tedone**[7] | **Luca Valle**[7] | **Margherita Moriero**[1,2] | **Daniela Verzola**[1] | **Fabrizio Montecucco**[1,2] | **Federico Carbone**[1,2]

[1]Department of Internal Medicine, University of Genoa, Genoa, Italy

[2]IRCCS Ospedale Policlinico San Martino, Genoa – Italian Cardiovascular Network, Genoa, Italy

[3]Molecular Pathology Unit, IRCCS Ospedale Policlinico San Martino, Genoa, Italy

[4]Department of Experimental Medicine, University of Genoa, Genoa, Italy

[5]Interventional Pulmonary Unit, IRCCS Ospedale Policlinico San Martino, Genoa, Italy

[6]Anatomic Pathology Unit, Department of Surgical Science and Integrated Diagnostics (DISC), University of Genoa, Genoa, Italy

[7]Anatomic Pathology Unit, Molecular Pathology Unit, IRCCS Ospedale Policlinico San Martino, Genoa, Italy

Correspondence
Federico Carbone, First Clinic of Internal Medicine, Department of Internal Medicine, University of Genoa, 6 Viale Benedetto XV, 16132 Genoa, Italy.
Email: federico.carbone@unige.it

Funding information
Ministero dell'Università e della

Abstract

Background: Interstitial lung diseases (ILDs) are characterized by progressive fibrosis, in which extracellular matrix remodelling is regulated by matrix metalloproteinases (MMPs) and their inhibitors (TIMPs). The MMP-9/TIMP-1 balance has been implicated in fibrogenesis, but its role in human ILD remains incompletely defined. This study aimed to assess the MMP-9/TIMP-1 ratio in BAL fluids of ILD patients, its relationship with fibrotic severity, and the cellular contribution of fibroblasts/myofibroblasts.

Methods: BAL samples from 48 consecutive ILD patients (non-fibrotic ILD, fibrotic ILD, idiopathic pulmonary fibrosis [IPF]) were analysed. MMP-9 and TIMP-1 concentrations were quantified by enzyme-linked immunosorbent assay (ELISA), and MMP-9 activity assessed by gelatin zymography. Fibroblasts/myofibroblasts were isolated from BAL of ILD patients and tested for TIMP-1 and MMP-9 release by ELISA, or protein expression by immunofluorescence. Published single-cell RNA sequencing datasets were reanalyzed (DESeq2 model) to define the cellular source of MMP-9 and TIMP-1.

Results: The MMP-9/TIMP-1 ratio was significantly reduced in BAL of patients with more advanced fibrosis, correlating with a higher presence of fibroblastic foci ($p = .002$) and collagen deposition ($p < .001$). This reduction was driven by both decreased MMP-9 and increased TIMP-1 levels. Zymography confirmed declining MMP-9 enzymatic activity across ILD subgroups. Fibroblasts, derived from BAL of ILD patients, displayed high TIMP-1 secretion but minimal MMP-9 release, consistent with their expression in immunofluorescence. Reanalysis of two independent scRNA-seq datasets confirmed predominant

Maria Bertolotto and Daniela de Totero are equally contributed as first authors of the present work.

Ricerca, Grant/Award Number: PE0000006; Ministero della Salute, Grant/Award Number: RCR-2022-23682288

TIMP-1 expression in fibroblast/myofibroblast clusters, with low but detectable MMP-9 expression.

Conclusions: Fibroblast-driven MMP-9/TIMP-1 imbalance in BAL reflects fibrotic severity in ILD. The MMP-9/TIMP-1 ratio may represent a supportive biomarker for differential diagnosis and phenotyping of ILD, warranting validation in larger multicenter studies.

KEYWORDS

extracellular matrix, interstitial lung disease, metalloproteasis, pulmonary fibrosis

1 | INTRODUCTION

The term interstitial lung diseases (ILDs) comprises a heterogeneous group of parenchymal lung disorders characterized by inflammation of the lung interstitium, each associated with different, albeit often unclear causes.[1] A subset of ILD patients develops a progressive fibrosing phenotype, sometimes meeting the criteria for idiopathic pulmonary fibrosis (IPF), a prototypical ILD in terms of pathogenesis and clinical behaviour.[2] Triggered by alveolar epithelial damage, fibroblast proliferation fuels the fibrotic process and represents a hallmark of fibro-proliferative ILDs. The differentiation of fibroblast into myofibroblast and subsequent collagen deposition are tightly regulated, rate-limiting steps in this process.

Zinc-dependent endopeptidase matrix metalloproteinases (MMPs) maintain the dynamic balance between extracellular matrix (ECM) production and degradation,[3] under the upstream control of specific inhibitors (namely tissue inhibitors of metalloproteinases [TIMPs]). Classes of MMPs and TIMPs are commonly found both in the bronchoalveolar lavage (BAL) and sera of patients with ILDs.[4–6] While the imbalance in MMP-9/TIMP-1 ratio theoretically accounts for lung fibrosis – supported by existing evidence[7,8] – the enzymatic activity of MMPs still lacks a detailed description. Molecular modelling studies have indeed recently identified distinct MMP-9/TIMP-1 complexes, exhibiting both inhibitory and non-inhibitory properties.[9]

Two anti-fibrotic agents, pirfenidone and nintedanib, are currently approved for the treatment of IPF and nintedanib for progressive fibrosing phenotype as well.[10,11] While their role is currently limited to reducing the progression rate of ILDs, recent evidence is extending the applications of nintedanib to the prevention[12,13] and even treatment of lung cancers in patients with ILDs.[14,15] Any progress in this field, including therapeutic approaches, could then be of paramount relevance for clinical practice. In this study, we analysed the levels of MMP-9 and TIMP-1 in BAL fluids from 48 ILD patients to refine disease categorization across ILD patterns, fibrosis severity and lung function. Particular focus was given to the MMP-9/TIMP-1 ratio, integrating complementary experimental (enzyme-linked immunosorbent assay [ELISA], zymography, fibroblast cultures, immunofluorescence) and bioinformatic (single-cell RNA sequencing [scRNA-seq] reanalysis) approaches.

2 | MATERIALS AND METHODS

2.1 | Study protocol, bronchoalveolar fluid collection and histological sample assessment

The present protocol has been approved by the Regional Ethics Committee (protocol code ILDFIBRO020, n. of Register CER Liguria: 523/2020 DB id 10,931) and has consecutively enrolled 48 patients with ILDs. Given the rarity of ILDs, the single center design and the exploratory nature of this study, no a priori power calculation was performed. Subgroup sizes reflect the real-world distribution of ILD patterns and subgroup comparisons are to be interpreted as hypothesis-generating. While IPF was defined according to international criteria,[16] the diagnostic workup for ILD involved discussion in a dedicated multidisciplinary group as well as trans-bronchial cryobiopsy and bronchoalveolar lavage (BAL) with diagnostic purposes[17]; ILDs were then radiologically categorized into non-fibrotic and fibrotic subtypes (Table S1). All samples were anonymised, and patients provided explicit authorization for their use in scientific research. Furthermore, total lung capacity (TLC), forced vital capacity (FVC), forced expiratory volume in 1 s (FEV1) and diffusing capacity (DLCO) were measured according to international guidelines and here reported as %.[18]

For histological analyses, all samples obtained by cryoprobing were fixed in formalin, routinely processed, embedded in paraffin, microtome cut, obtaining three

levels of sections that were subsequently stained with haematoxylin and eosin. Adjunctive histochemical staining (Alcian blue PAS and Mallory's trichrome) and immunohistochemistry (Cytokeratin 7, all provided by Ventana Medical System, Inc., Oro Valley, AZ) were performed to facilitate the diagnostic process. Determination and scoring evaluation of the presence of fibroblastic foci and of collagen fibrosis was given based on previous literature.[19,20]

2.2 | Fibroblast isolation and in vitro culture

For bronchoalveolar lavage (BAL), 50 mL aliquots of sterile physiological saline at room temperature were instilled and gently aspirated 3–4 times, for a total volume not exceeding 200 mL. An adequate return, defined as ≥30% of the instilled volume, was required, with 15–20 mL used for cellular analyses; this corresponded to the small fraction usually left unused after routine diagnostic analyses. Cells from BAL fluids were pelleted by centrifugation, recovered and seeded in 24-well plates with 1 mL of culture medium. They were cultured and expanded in vitro in RPMI-1640 medium supplemented with 10% fetal calf serum (FCS) and 100 U/mL penicillin–streptomycin (Euroclone, Milan, Italy), at 37°C in a humidified atmosphere containing 5% CO_2.[21] Recombinant human fibroblast growth factor-2 (FGF2, Miltenyi Biotech GmbH, Bergisch-Gladbach, Germany) was added at a sub-optimal concentration of 3 ng/mL, starting 1 day after plating and re-added once a week. When fibroblasts reached confluence, cells were detached with trypsin (Euroclone) and replated in new wells or flasks for further expansion. Supernatants of cultured fibroblasts were collected when cells were nearly confluent and maintained without FGF2 before harvesting. Fibroblasts could be successfully derived from BAL samples of 10 ILD patients out of 48 processed, while no viable fibroblasts were obtained from the few BAL samples received as controls. This limitation reflects both the technical and ethical challenges of isolating viable fibroblasts from BAL in individuals without pulmonary disease, since bronchoalveolar lavage is rarely performed in healthy subjects and fibroblast outgrowth efficiency from such samples is intrinsically low. Therefore, for control conditions used in a subset of experiments, we cultured and derived supernatants from the MRC5 and HFFF2 fibroblast cell lines (Biobank 'Interlab Cell Line Collection,' IRCCS Ospedale Policlinico San Martino, Genoa, Italy) and from primary skin fibroblasts obtained from a healthy donor. MRC5 and HFFF2 cell lines were maintained in RPMI-1640 medium supplemented with 10% FCS, whereas skin fibroblasts were expanded in the same medium with the addition of FGF2. All fibroblast cultures used in the experiments had been previously characterized for the expression of mesenchymal and fibroblast markers, including CD105, CD90, CD73, fibronectin, collagen I and α-smooth muscle actin (α-SMA), as previously described.[21–23]

2.3 | MMP-9 and TIMP-1 determination in BAL from ILDs patients

MMP- 9 and TIMP-1 were measured via colorimetric enzyme-linked immunosorbent assay (ELISA), following manufacturer's instructions (DuoSet, R&D Systems), Supernatants of fibroblasts derived from some ILD patients and cultured in vitro were also assayed. The lower limit of detection was 31.25 pg/mL for MMP-9 and 46.88 pg/mL for TIMP-1.[24,25] MMP-9 and TIMP-1 concentrations were measured on raw BAL supernatants without normalization to total protein, as the recovered volumes and total protein content showed minimal variability across samples and ILD subgroups. Protein concentration, within the recovered volumes of BAL volumes, was assessed by the BCA enhanced methods, according to the manufacturer's suggestions (Thermo Fisher Scientific, Waltham, MA; product #23227; PierceTM BCA Protein Assay Kit).

2.4 | Evaluation of pro-MMP-9 activity by gelatin zymography

Gelatin zymography was here applied for the quantitative measurement of pro-MMP-9 activities. Equal amounts of samples (30 μL) and 1 ng of recombinant pro-MMP-9 standard (Calbiochem, Lucern, Switzerland) were loaded on 9% sodium dodecyl sulfate (SDS)-polyacrylamide gels copolymerized with gelatine (Sigma-Aldrich, St. Louis, MO) without any reducing agent. These gels were then rinsed and stained with Coomassie Blue R-250 (Thermo Fisher Scientific, Waltham, MA). The results of zymography were expressed as pro-MMP-9 proteolytic activity according to the formula: supernatant pro-MMP-9 $= (I_{obs}/I_{std}) \times W_{std}$. I_{obs} and I_{std} refer to the intensities of gelatinolytic areas produced by samples and pro-MMP-9 standard, respectively; W_{std} is the reference weight (1 ng) of the loaded pro-MMP-9 standard. Pro-MMP-9 activity was expressed as $ng \times mL^{-1}$. Gelatinolytic bands were measured with a gel analysis system (GeneGenius, Syngene, Cambridge, UK).[26,27] BAL samples from ILD patients were analysed according to material availability: 10 from the non-fibrotic group, 9 from the fibrotic group and 17

from the IPF group. For greater accuracy of the analysis, 8 additional control BAL samples were obtained from subjects undergoing bronchoscopy for non-ILD conditions (Table S1).

2.5 | Immunofluorescence staining

Immunofluorescence staining was performed on fibroblasts derived from ILD patients and grown in chamber slides (Thermo Fisher Scientific). Once fixed with 2% paraformaldehyde and treated with Triton X-100, the cells were incubated overnight with an anti-human TIMP-1 antibody and anti-human MMP-9 polyAb antibody (all from R&D Systems Minneapolis, MN).[28] Primary monoclonal antibodies were prepared with 1% bovine serum albumin (BSA) as a blocking solution. Fibroblasts were then stained with a goat anti-mouse Alexa Fluor 488 (Invitrogen, Life Technologies, Carlsbad, CA) or anti-goat PE-conjugated secondary antibodies (Southern Biotechnology, Birmingham, AL). Cell nuclei were further identified by standard staining with 4′,6-diamidino-2-phenylindole dihydrochloride (DAPI; Merck Serono S.p.A., Rome, Italy). Images were captured at 40x magnification with the appropriate white balance set according to the fluorescence filter.

2.6 | Gene Expression Profile Analysis from Deposited Single Cell RNA Datasets

Single cell RNA UMI (Unique Molecular Identifiers) count matrices were retrieved from the Gene Expression Omnibus (GEO) GSE136831 (Naftali Kaminski)[29] and GSE135893 (Nicholas Banovich)[30] repositories; specifically, only down-sampled matrices encompassing annotated cells meeting single-cell sequencing quality criteria were deemed as appropriate for further differential expression analysis. Down-samples UMI count matrices were normalized by means of the 'NormalizeData' function, encompassed in the Seurat R package,[30–35] set to 'LogNormalize' setting: briefly, each gene feature UMI count was divided by the total number of gene features assayed, scaled by a factor of 10,000 and log2-transformed. Prior to the previous step, cell expression profile were merged, for each patient, according to the re-annotation specified in the legend of Figures 4 and 5, calculating pseudo-bulk expression profiles. A DESeq2 model[36] was fitted to the bulk expression profile matrices for each GSE dataset with the following gene filtering criteria: gene read count sum across samples less than 10, in at least three pseudo-bulk samples. In order to test the coefficient contrast significance of target genes TIMP-1 and MMP-9, the adjusted p-value threshold was set to .05. Contrasts were formulated between the "Fibroblast" and "Myofibroblast" classes and against each of them to the re-annotated classes.

2.7 | Statistical analysis

R Core Team (2021). R: A language and environment for statistical computing (R Foundation for Statistical Computing, Vienna, Austria. URL https://www.R-project.org/) and GraphPad Prism version 10.3.1 (GraphPad Software, Inc., La Jolla, CA) were used for statistical analysis. Clinical data were reported as absolute and relative frequencies when categorical, and comparisons drawn by Fisher's exact test, as appropriate. As the normality assumption—tested by Shapiro–Wilk—was not demonstrated, continuous clinical variables were presented as median and interquartile range (IQR) and intergroup comparisons drawn by Mann–Whitney, Kruskal-Wallis, or Jonckheere-Terpstra tests, as appropriate. To address potential confounding by age and treatment, continuous outcomes (pulmonary function tests) were analysed using analysis of covariance (ANCOVA), with ILD pattern as the fixed factor and age and systemic corticosteroid use entered as covariates. Adjusted pairwise differences between ILD groups were derived from estimated marginal means with Tukey correction for multiple comparisons. Biomarkers (MMP-9, TIMP-1 and the MMP-9/TIMP-1 ratio) were modelled within the same framework. Histological features (fibroblastic foci and collagen fibrosis) were analysed as ordinal outcomes using proportional odds regression with the same covariate structure (pattern, age, corticosteroid use). Conversely, to test the prognostic effect of histology, both foci and collagen fibrosis were also modelled as predictors of pulmonary function indices and biomarkers (linear regression for continuous outcomes), with and without adjustment for age and corticosteroids. For each model we systematically reported: (i) the crude effect of the main predictor (pattern or histology); (ii) the adjusted effect after including age and corticosteroid use; (iii) the likelihood-ratio or F-test evaluating improvement in model fit with added covariates; and (iv) formal interaction terms between pattern/histology and covariates. In addition, Tukey-adjusted pairwise contrasts were computed not only for ILD patterns but also for histological levels (foci and collagen fibrosis) to quantify differences across ordered categories. For all comparisons a p-value $<.05$ was set as statistically significant. Statistical methods applied to interrogate single cell RNA sequencing data are described in the related article section 'Gene Expression Profile Analysis from Deposited Single Cell RNA Datasets'.

TABLE 1 Descriptive statistics.

Variable	Overall cohort ($n=48$)	Pattern		
		Non-fibrotic PID ($n=14$)	Fibrotic PID ($n=10$)	IPF ($n=24$)
Sex, male	34 (70.8)	7 (50.0)	8 (80.0)	19 (79.2)
Age, y	75 [64–78]	64 [60–72]	73 [61–78]	77 [74–79]
Smoke habit				
Never	17 (35.4)	6 (42.9)	3 (30.0)	8 (33.3)
Former	30 (62.5)	7 (50.0)	7 (70.0)	10 (66.7)
Active	1 (2.1)	1 (5.8)	0 (.0)	0 (.0)
Asthma, *n* (%)	4 (8.3)	1 (7.14)	1 (10.0)	2 (8.3)
COPD, y *n* (%)	4 (8.3)	2 (14.3)	1 (10.0)	1 (4.2)
Allergic rhinitis/conjunctivitis, *n* (%)	3 (6.3)	2 (14.3)	0 (.0)	1 (4.2)
Myocardial disease, *n* (%)	7 (14.6)	2 (14.3)	1 (10.0)	4 (16.7)
Former malignancy, *n* (%)	9 (18.8)	2 (14.3)	1 (10.0)	6 (25.0)
Hypertension, *n* (%)	23 (47.9)	2 (14.3)	8 (80.0)	13 (54.2)
Diabetes, *n* (%)	7 (14.6)	2 (14.3)	3 (30.0)	2 (8.33)
Hiatal hernia, *n* (%)	4 (8.3)	0 (.0)	1 (10.0)	3 (12.5)
Autoimmune disease, *n* (%)	6 (12.5)	2 (14.3)	3 (30.0)	1 (4.2)
ANA positivity, *n* (%)	21 (43.8)	9 (64.3)	6 (60.0)	6 (25.0)
ENA positivity, *n* (%)	4 (8.3)	2 (14.3)	0 (.0)	2 (8.3)
SS antibodies, *n* (%)	2 (4.2)	2 (14.3)	0 (.0)	0 (.0)
Echocardiographic pulmonary hypertension, *n* (%)	13 (39.4)	2 (14.3)	3 (30.0)	8 (33.3)
WBC count, cells/mm^3	6.7 [5.8–8.0]	[6.4–8.5]	7.7 [6.5–10.3]	6.2 [5.6–7.4]
Neutrophil count, cells/mm^3	3.7 [3.3–4.4]	3.8 [3.7–5.7]	4.0 [3.4–5.3]	3.6 [3.1–4.0]

Note: Continuous variables are presented as absolute (relative) frequencies; continuous ones are summarized as median [interquartile range].

Abbreviations: ANA, anti-nucleus antigen; COPD, chronic obstructive pulmonary disease; ENA, extractable nuclear antigen; SS, systemic sclerosis; WBC, white blood cells.

3 | RESULTS

3.1 | Clinical characteristics of the ILDs patients

Clinical details of the 48 patients included in the present study (overall and categorized across ILD patterns) are summarized in Table 1 and Table S1. Diagnosis relied on a combination of clinical evaluation, high-resolution chest CT scan, BAL and tissue sampling, multidisciplinary discussion. As mentioned above, patients were categorized as: non-fibrotic/progressive fibrotic, and IPF. As expected, histology showed strong differences across patterns: fibroblastic foci and collagen fibrosis were significantly more prevalent in fibrotic ILD and IPF ($p<.01$ for all comparisons) (Figure 1A), and these associations remained unchanged after adjustment for age and corticosteroid use. Age differed significantly across ILD patterns ($p=.004$ for trend), with IPF patients being older than those with non-fibrotic ILD (Tukey $p=.004$). In unadjusted analyses, more fibrotic phenotypes exhibited lower FVC% ($p=.037$) and FEV1% ($p=.017$). However, after adjustment for age and corticosteroid use, these associations were attenuated and no longer significant (FVC% $p=.095$; FEV1% $p=.236$) (Table S2). Similarly, TLC% and DLCO% showed no significant pattern-related differences in adjusted models. Pairwise comparisons confirmed these findings, with mean FVC% differences of +8.9 (−8.4 to 26.2) between non-fibrotic and fibrotic ILD ($p=.43$) and −11.0 (−26.9 to 4.9) between fibrotic ILD and IPF ($p=.23$) (Table S3).

When histological remodelling was considered, fibroblastic foci were associated with reduced DLCO% (adjusted $p=.021$) (Table S3). Increasing collagen fibrosis was consistently associated with impaired pulmonary function, including lower FEV1% (adjusted $p=.590$; LR/F test = .005), reduced FVC% (adjusted $p=.681$; LR/F test = .004) and lower FVC/FEV1 ratio (adjusted $p=.699$; LR/F test = .013) (Table S2). These findings indicate that histological severity contributes to functional decline beyond demographic and treatment confounders.

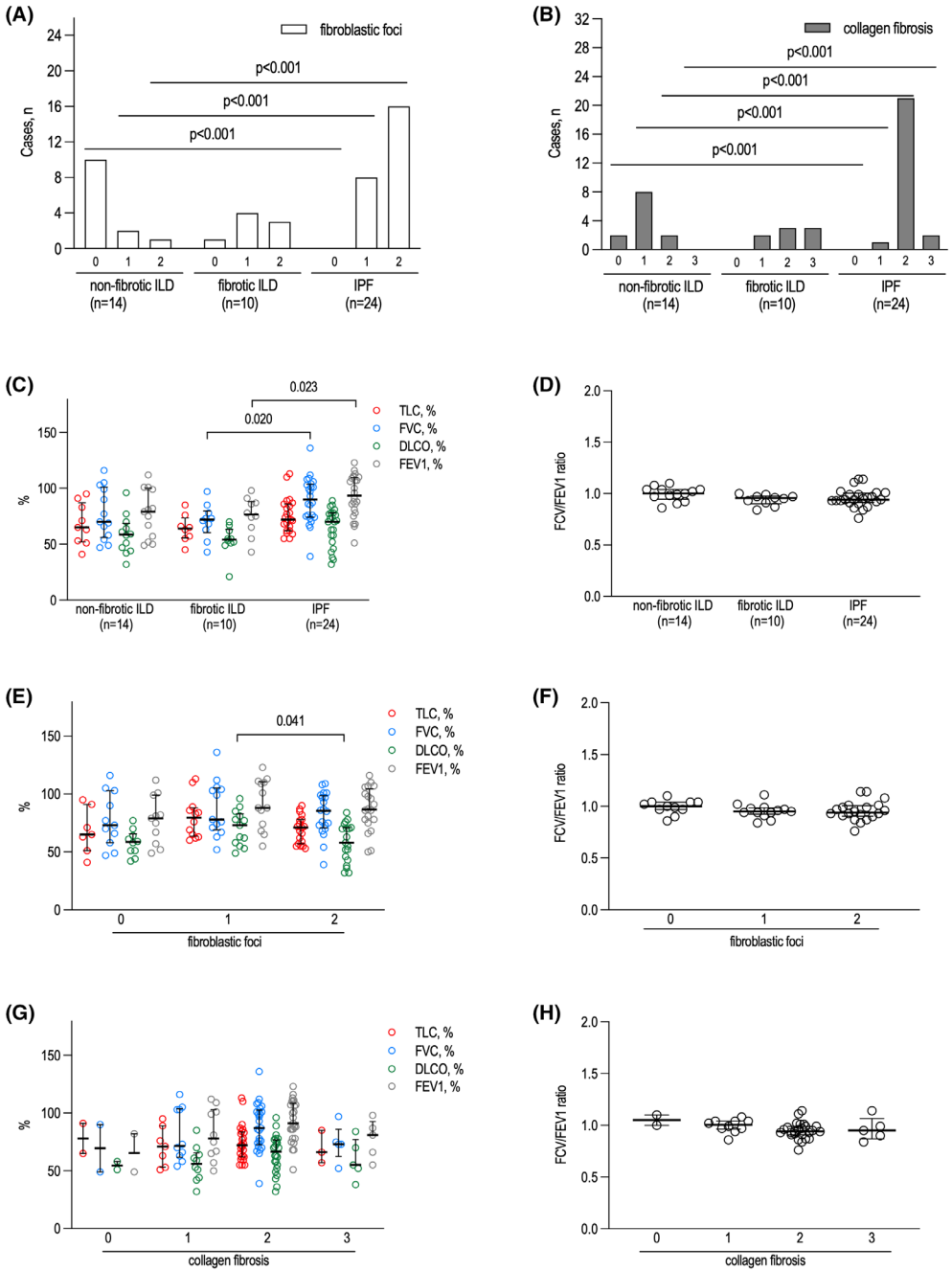

FIGURE 1 Patterns of interstitial lung diseases (ILDs: Non-fibrotic, fibrotic and idiopathic pulmonary fibrosis [IPF]) are related to fibrosis and functional features. Fibroblastic foci (A) and collagen fibrosis (B) are differentially expressed across ILDs patterns. A semi-quantitative distribution is reported according to the distribution of fibrosis (x-axis score 0–2; panel A) and fibroblastic foci (x-axis score 0–3; panel B). Patterns of ILDs are also differently associated with physiologic indices of lung function: Total lung capacity (TLC, % predicted), forced vital capacity (FVC, % predicted), diffusing capacity for carbon monoxide (DLCO, % predicted), forced expiratory volume in 1 s (FEV1, % predicted), and the ratio between FVC/FEV1 (C–H). *p*-values for panel (A and B) are reported numerically and refer to group comparisons by Kruskal–Wallis with post-hoc testing; for panel (C–H) *p*-values refer to intergroup comparisons.

3.2 | The MMP-9/TIMP-1 ratio differs significantly in the bronchoalveolar lavage from different ILD patterns

In BAL fluid from 48 ILD patients, MMP-9 concentrations decreased across fibrotic phenotypes (*p*-for-trend .048; Figure 2A) and histologic grades (*p*-for-trend .008 for fibroblastic foci and .004 for collagen fibrosis; Figure 2C,E), while TIMP-1 decreased with increasing collagen fibrosis ($p = .004$). Consequently, the MMP-9/TIMP-1 ratio decreased progressively from non-fibrotic toward fibrotic ILD and IPF (*p*-for-trend .030; Figure 2B) and declined

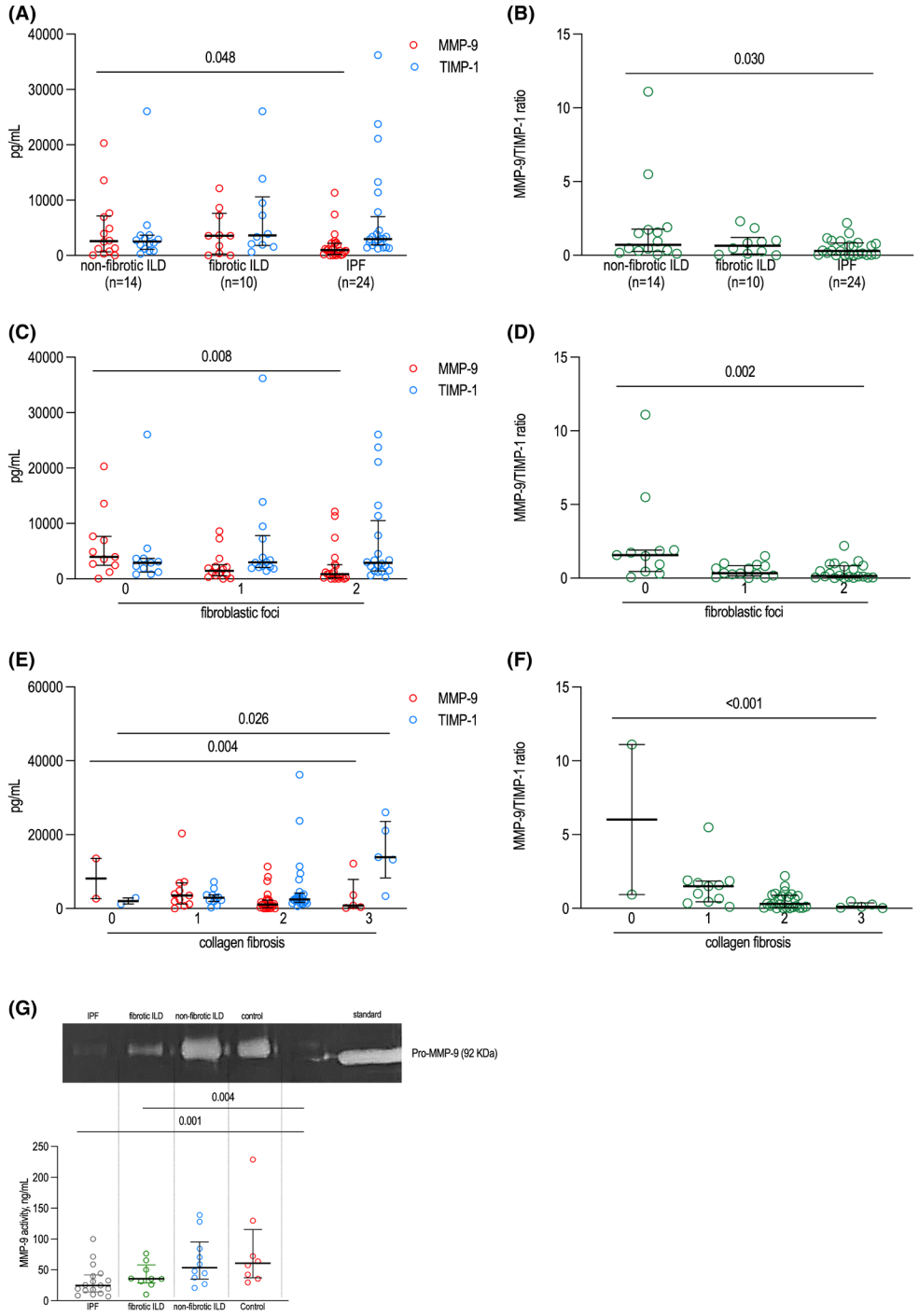

FIGURE 2 Matrix metalloproteinase (MMP)-9 and its inhibitor TIMP-1 are differentially expressed across ILD patterns and according to fibrosis severity. Panel (A) shows individual concentrations of MMP-9 (red) and TIMP-1 (blue) in non-fibrotic ILD, fibrotic ILD and idiopathic pulmonary fibrosis (IPF), while panel (B) illustrates the corresponding MMP-9/TIMP-1 ratio across the same groups. Panels (C and D) depict MMP-9 and TIMP-1 concentrations (C) and the MMP-9/TIMP-1 ratio (D) stratified by fibroblastic foci score (0–2), whereas panels (E and F) show the same parameters stratified by collagen fibrosis score (0–3). The bottom panel presents gelatin zymography results, demonstrating pro-MMP-9 (~92 kDa) and quantification of its enzymatic activity (ng/mL) in BAL fluids from IPF ($n = 17$), fibrotic ILD ($n = 9$), non-fibrotic ILD ($n = 10$) and controls ($n = 8$, obtained from subjects undergoing bronchoscopy for non-ILD conditions). Data are expressed as medians with interquartile ranges. p values, calculated using Kruskal–Wallis with Dunn's post-hoc test or Mann–Whitney test where appropriate, are reported numerically above the brackets.

with both fibroblastic foci (p-for-trend <.001) and collagen fibrosis severity (p-for-trend <.001). Adjustment for age and corticosteroid use confirmed these overall trends. In models adjusted for age and corticosteroid use, MMP-9 concentrations and the MMP-9/TIMP-1 ratio both decreased significantly across ILD patterns and histologic grades (adjusted $p = .028$ for the ratio; $p = .005$ for TIMP-1 with collagen fibrosis), whereas no significant interaction effects were observed (Table S2). At pairwise adjusted comparisons, some contrasts reached statistical significance, although the overall effect of ILD pattern was modest (Table S3).

In gelatin zymography, performed to confirm a differential activity of MMP-9 in BAL fluids, the extent of its matrix degradation decreased as fibrosis progressed through the different ILD patterns, with the highest values observed in non-fibrotic ILDs, and controls as well ($p = .004$ for fibrotic ILD and .001 for IPF; p-for-trend .002) (Figure 2D).

Fibroblasts derived from BAL of ILD patients ($n = 10$) showed a secretory phenotype characterized by the production of TIMP-1, but not MMP-9, at very high concentrations (p-value = .002 and .343, respectively) while fibroblasts from control subjects (included for exploratory comparison) released TIMP-1 at lower concentrations (almost threefold lower) (Figure 3A,B). Consistent with the MMP-9 and TIMP-1 measurements, ILD fibroblasts were positive for MMP-9 and TIMP-1 expression by immunofluorescence analysis (Figure 3C). This potential involvement of fibroblasts is further suggested by the lack of any other correlation of the other cell types found within the BAL (e.g. macrophages, lymphocytes and neutrophils) with cytokine release or lung function tests (Figure S1). Rather, fibroblast-associated features, including the fibroblastic foci and collagen fibrosis scores, further exhibited a consistent and significant association with markers of lung injury and with cytokine secretion levels.

3.3 | Evaluation of TIMP-1 and MMP-9 expressions on different pulmonary sub-types by lung single cell RNA sequencing analysis

To confirm whether the imbalance between TIMP-1 and MMP-9 detected in the BAL from ILD patients could be really related to fibroblasts/myofibroblasts expansion, we explored and analysed two gene expression profile datasets published and deposited by Kaminski/Rosas (GSE136831)[29] and Banovich/Kropsky (GSE135893).[30] By single cells RNA sequencing, Kaminski and Rosas have analysed samples derived from: IPF ($n = 32$), chronic obstructive pulmonary disease (COPD) ($n = 18$), sand controls ($n = 29$), while Banovich and Kropsky analysed cells from 20 patients with ILDs (12 with IPF, 2 with chronic hypersensitivity pneumonitis, 3 with non-specific interstitial pneumonia, 2 with sarcoidosis and one unclassifiable ILD) and 10 controls. Figures 4A and 5A display how fibroblasts/myofibroblasts retain the highest expression of TIMP-1 in both datasets. TIMP-1 is well expressed by monocytes/macrophages but at lower levels, whereas MMP-9 expression is ubiquitously reduced. Moreover, trying to better define and quantify the levels of TIMP-1 in different subpopulations composing the lung parenchyma, we have examined raw data derived from the two above reported databases. Even excluding COPD (Kaminski/Rosas)[29] or pooling ILDs repositories (Banovich/Kropsky), we confirm that, by single cell RNA sequencing transcriptional TIMP-1 levels are significantly higher in fibroblasts/myofibroblasts as compared to the other lung cell types (Figures 4B and 5B). When MMP-9 was filtered from both queried datasets before the DESeq2 model fitting, its low expression among the compared cell types did not meet the designated read count sum threshold, as previously specified in the Section 2. To further clarify this point, we repeated the analysis with relaxed gene-filtering criteria, only considering a read count sum <5. After this reanalysis, single-cell data from both Kaminski (GSE136831) and Banovich (GSE135893) cohorts again showed significant TIMP-1 enrichment in fibroblast/myofibroblast clusters, whereas MMP-9 expression remained low in cellular representation and non-significant across comparisons (Figure S2). The paucity of MMP-9 signal in these public scRNA-seq resources likely reflects both biologically low/inducible expression and dataset-specific technical sparsity. Consistency with our BAL ELISA, zymography and fibroblast culture data supports the conclusion that TIMP-1-driven imbalance is a key feature of fibrotic ILD.

4 | DISCUSSION

In the present study, we provide new insights into the role of MMP-9/TIMP-1 imbalance in ILDs. Very high TIMP-1 concentrations coupled with low levels of MMP-9 in the BAL from ILD patients, are associated with a prevalent fibrotic pattern, consistent with the presence of fibroblastic foci and the degree of collagen fibrosis. This observation is somewhat confirmatory of the diagnostic potential of BAL in the workup of ILDs.[37] An extensive, albeit debated, literature describes clinical scenarios for its use, especially in discriminating between ILD phenotypes, assessing treatment response and excluding alternative diagnoses (e.g. infectious processes, cryptogenic organizing pneumonia, extrinsic allergic alveolitis and connective tissue disease−/respiratory bronchiolitis-associated

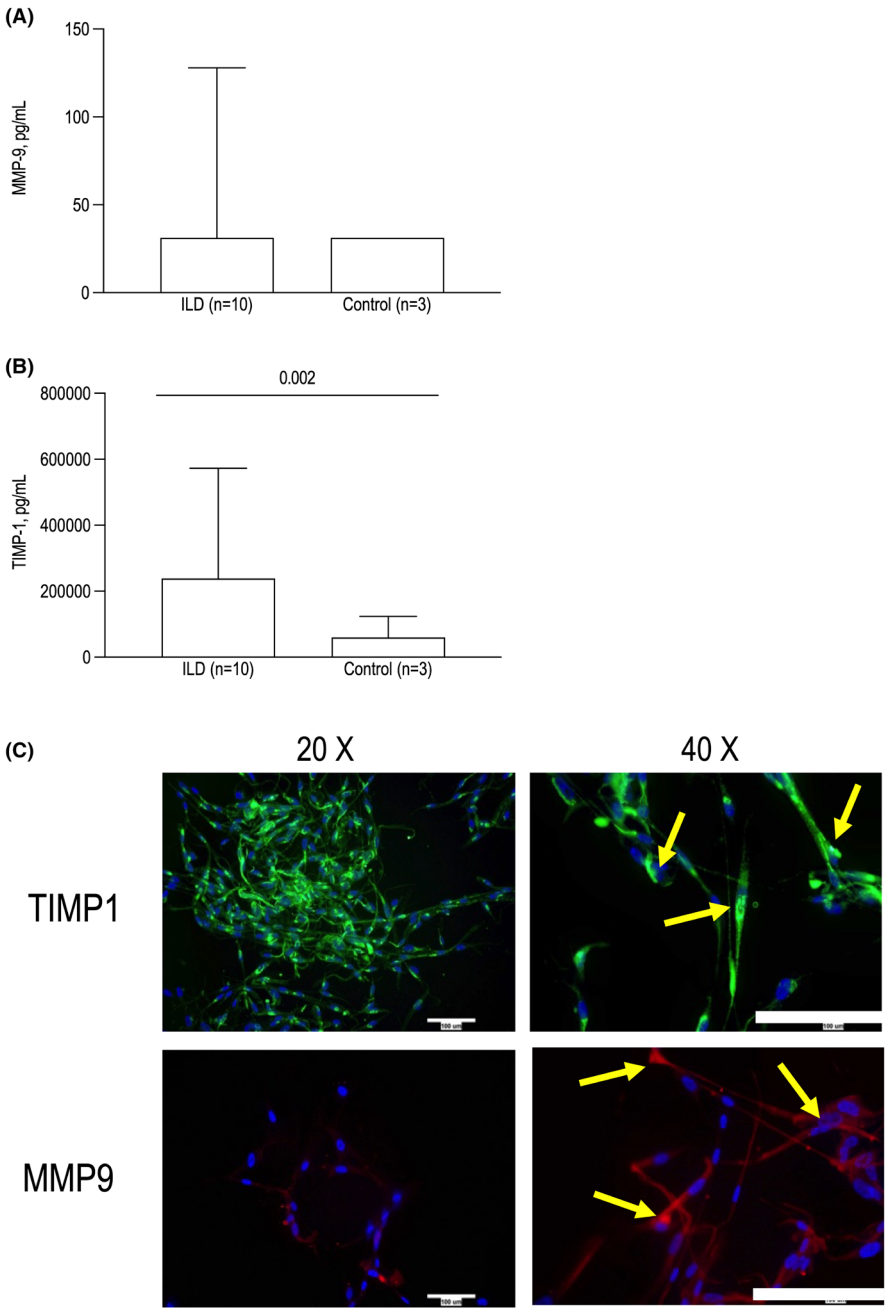

FIGURE 3 Primary lung fibroblasts from ILD patients secrete more TIMP-1 than controls. In fibroblasts derived from ILD-patients ($n = 10$) and cultured in vitro concentrations of not MMP-9 (A) but TIMP-1 ($p = .022$) (B) are significantly higher than controls ($n = 3$). Boxes show median with IQR, whereas indicate the range. Panel (C) is representative of immunofluorescence images from fibroblasts stained for TIMP-1 (green) and MMP-9 (red). Images magnified at 20× and 40×, with the scale bar corresponding to 100 μM.

ILD).[38–40] In the context of ILDs, BAL reflects the severity of lung injury and even performs on outcome prediction.[41] However, this minimally invasive procedure likely has the potential to be more informative than it currently is. In the '-omics era', BAL is still interrogated mainly for its cellular but poorly for its molecular composition.[42,43]

Nevertheless, MMPs and their inhibitors (TIMPs) have an established role in polarizing ECM remodelling toward fibrosis in lung injury.[8,9,44,45] Here, a prevalent release of TIMP-1 at very high levels in BAL, coupled with a decrease in MMP-9, characterizes more severe pulmonary fibrosis. Delving deeper, this imbalance in matrix homeostasis regulators increases with the number of fibroblastic foci and the ratio of collagen fibrosis. In vitro experiments – confirmed by data from two different single-cell RNAseq atlases – suggest how fibroblasts/myofibroblasts might

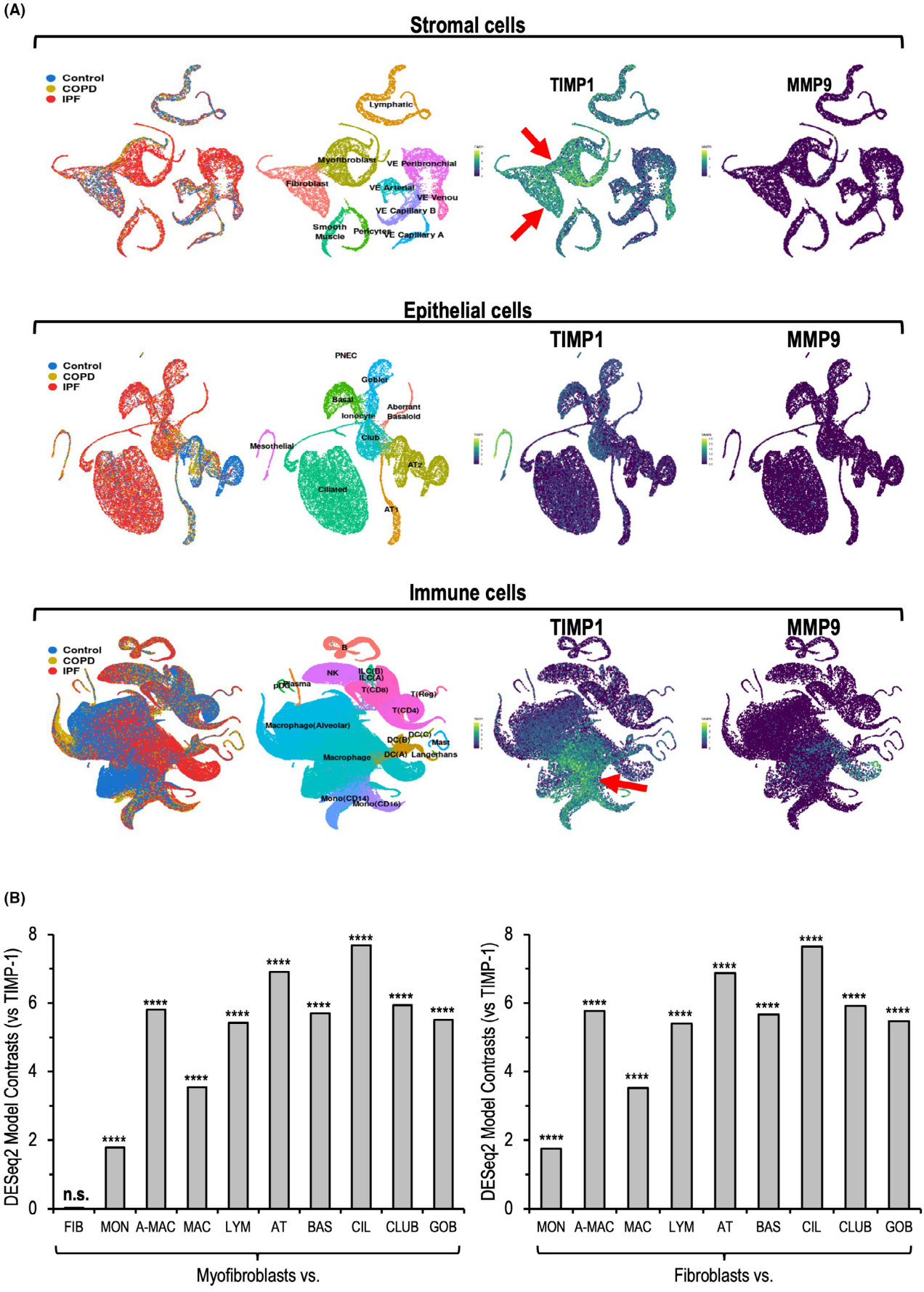

FIGURE 4 RNA sequencing from Kaminski/Rosas (GSE136831) repository. From the Uniform Manifold Approximation and Projection (UMAP) here displayed it is evident that the highest TIMP-1 expression is retained by fibroblasts/myofibroblasts as compared to the other lung cell types (A), as confirmed by the DESeq2 model (B). Evaluation of TIMP1 mRNA expression in myofibroblasts and fibroblasts versus the others types of cells present in the lung. Reannotated classes: MYO, Myofibrolasts; FIB, Fibroblasts; MON, CMonocytes ncMonocytes; MAC, Macrophages; A-MAC, Alveolar macrophages; AT, Alveolar type I/II cells; CIL, Ciliated cells; CLUB, Club cells; GOB, Goblet cells; LYM, T cells (cytotoxic/regulatory), innate lymphoid cells (ILC) A/B, natural killer (NK) cells, B cells, plasma cells. ns: $p > .05$; *$p < .05$; **$p < .01$; ***$p < .005$; ****$p < .0005$.

contribute to the MMP9/TIMP-1 imbalance. While high levels of TIMP-1 have been widely detected in lung fibrosis from the transcriptional level to targeted immunoassay in BAL and serum,[46] the contribution of TIMP-1 to the pathogenesis of lung fibrosis has been variously demonstrated in experimental mice models.[47–49] Both TIMP-1 deletion and targeted therapies (e.g. bosentan) have indeed been shown to reverse the imbalance between MMP-9/TIMP-1 in parallel with reducing fibroblast proliferation, ECM deposition and ultimately lung fibrosis, potentially through the ERK (extracellular-signal-regulated kinase pathway) pathway activation mediated by the CD63/integrin β1.[8,50]

Far from being a dance for two, the differential expression and release of MMP-9 and TIMP-1 likely involve a complex cytokine storm within the lung microenvironment. Among them, the pro-fibrotic effect of TGF (transforming growth factor)-β, which couples with a TIMP-1 up-regulation, is well recognised. Similarly, the contribution of IL-33 to pro-fibrotic ECM remodelling in lung fibrosis is closely linked to an imbalance between MMP-9 and TIMP-1.[51] Some studies have also suggested a protective role for bone marrow-derived mesenchymal stem cells. Injection in bleomycin-treated mice indeed blunts epithelial injury and lung inflammation and normalizes myofibroblast activity, restoring a balance between MMPs and TIMPs.[52,53] It should finally be noted that TIMP-1 overexpression also occurs in tumour-associated fibroblasts in lung adenocarcinoma,[54] where it seems to have a potential prognostic relevance.[55]

Our findings align with current literature, supporting TIMP-1 overexpression as a key factor in fibroblast activation, polarisation and lung fibrosis. The MMP-9/TIMP-1 ratio in BAL may hold potential clinical relevance as a supportive tool in the differential diagnosis of ILD. The pronounced reduction in this ratio – driven by elevated TIMP-1 and reduced MMP-9 – was most evident in patients with idiopathic pulmonary fibrosis and advanced fibrotic ILD. This observation indicates that the ratio may serve as a molecular marker of fibrotic burden, complementing imaging and histopathological evaluation. Although not intended as a standalone diagnostic tool, incorporating the MMP-9/TIMP-1 ratio into a multimodal diagnostic approach could refine ILD phenotyping, aid in distinguishing progressive fibrotic forms from non-fibrotic patterns and ultimately support early therapeutic decision-making. Prospective and multicenter studies will be required to validate this potential and to determine the practical utility of the MMP-9/TIMP-1 ratio in clinical settings. On the other hand, we acknowledge that much remains to be understood regarding TIMP-1 biology in ILDs, and the present study retains several limitations. First, it was conducted in a monocentric, cross-sectional setting, which limits generalizability and precludes causal inference. Second, subgroup sizes were relatively small, particularly in the fibroblast control cohort, reflecting the rarity of ILD and the technical difficulty of obtaining viable fibroblast outgrowth from BAL samples of non-ILD individuals. Therefore, the in vitro results should be interpreted as qualitative evidence of cellular behaviour rather than as a quantitative comparison across ILD subtypes. Third, in the single-cell RNA sequencing analyses, MMP-9 expression was underrepresented, likely due to both biological factors (low and inducible expression) and technical thresholds applied during filtering. Fourth, our scRNA-seq findings rely on the reanalysis of publicly available datasets generated under heterogeneous experimental and clinical conditions, which may not fully correspond to our patient cohort; these data should therefore be considered supportive and hypothesis-generating. Finally, given the exploratory nature of the study, our results should be regarded as hypothesis-generating and warrant validation in larger, independent, multicenter cohorts with longitudinal follow-up.

In conclusion, we demonstrate that fibroblast-driven imbalance of the MMP-9/TIMP-1 axis in BAL reflects fibrotic severity across ILD patterns, with the most pronounced reduction observed in IPF. This identifies the BAL MMP-9/TIMP-1 ratio as a translational readout of extracellular matrix remodelling and a candidate supportive biomarker for ILD phenotyping and differential diagnosis. We are seeking future studies capable of delving deeper into TIMP-1 biology and confirming our observations on the direct correlation between imbalanced MMP-9/TIMP-1 expression and fibrotic progression in ILDs.[56] Before speculating on potential therapeutic applications, future studies should focus on developing tailored algorithms incorporating TIMP-1 to refine ILD phenotyping and prognostic risk stratification.

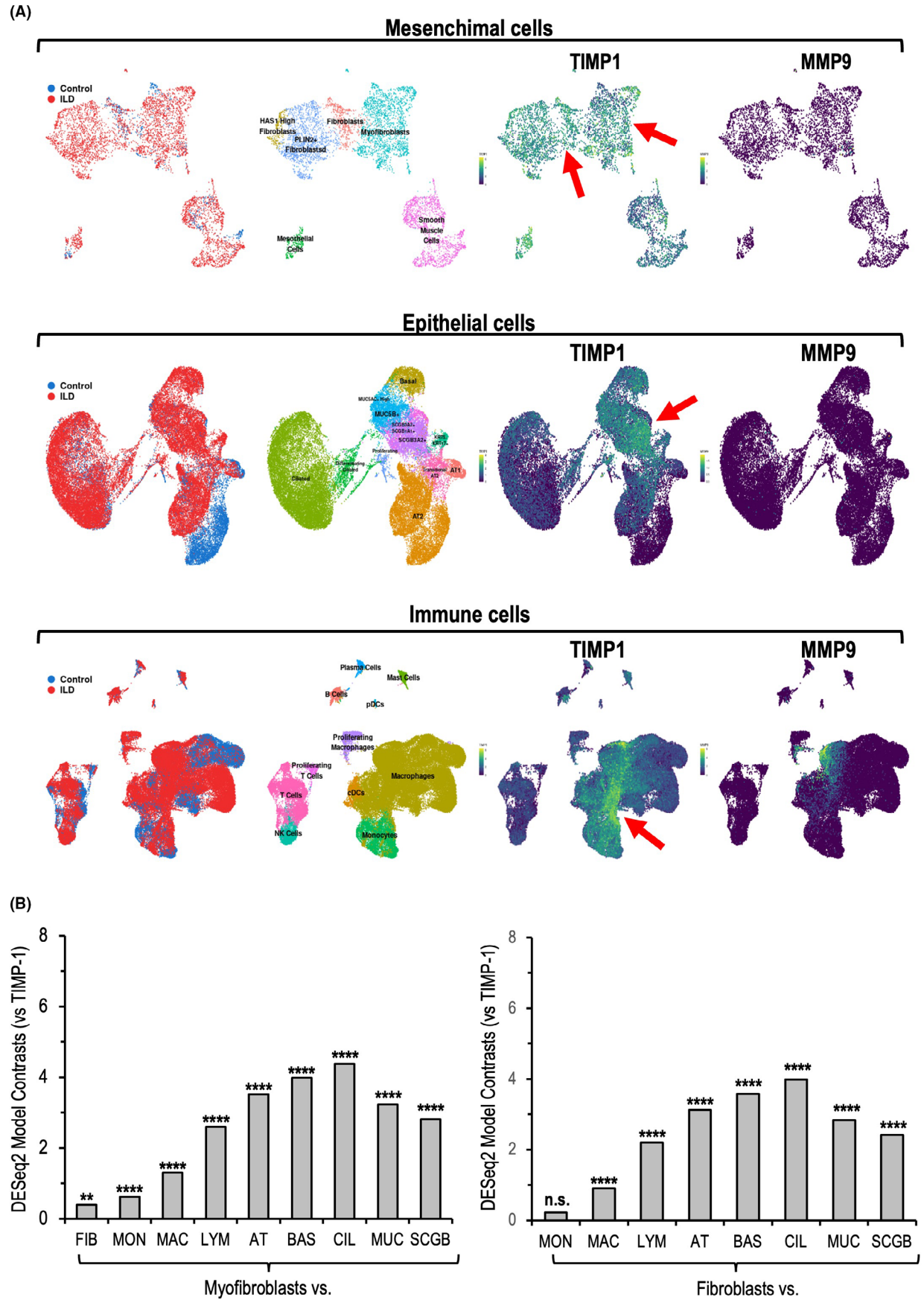

FIGURE 5 RNA sequencing from Banovich/Kropsky (GSE135893) repository. From the Uniform Manifold Approximation and Projection (UMAP) here displayed it is evident that the highest TIMP-1 expression is retained by fibroblasts/myofibroblasts as compared to the other lung cell types (A), as confirmed by the DESeq2 model (B). Evaluation of TIMP1 mRNA expression in myofibroblasts and fibroblasts versus the others types of cells present in the lung. Reannotated class: MYO, Myofibrolasts; FIB, Fibroblasts; MON, Monocytes; MAC, Macrophages; BAS, Basal cells; AT, AT I/II cells; CIL, Ciliated and differentiating ciliated cells; MUC, MUC5b/5AC+ cells; SCGB, SCGB3A2/1A13A2+ cells; LYM, T cells (cytotoxic/regulatory), innate lymphoid cells (ILC) A/B, natural killer (NK) cells, B cells, plasma cells. ns: $p > .05$; *$p < .05$; **$p < .01$; ***$p < .005$; ****$p < .0005$.

AUTHOR CONTRIBUTIONS

Conceptualization: Maria Bertolotto, Daniela de Totero. Methodology: Paolo Giannoni, Emanuela Barisione, Marco Grosso, Simona Pigozzi, Roberto Fiocca, Luca Valle, Elisabetta Tedone, Daniela Verzola. Investigation (clinical sampling, BAL procedures, laboratory experiments, histology): Emanuela Barisione, Marco Grosso, Daniela de Totero, Simona Pigozzi, Roberto Fiocca, Luca Valle, Paolo Giannoni, Maria Bertolotto. Data curation: Federico Carbone, Margherita Moriero, Maria Bertolotto. Formal analysis (statistics and data visualization): Federico Carbone, Ennio Nano. Resources: Fabrizio Montecucco, Daniela de Totero. Supervision: Fabrizio Montecucco, Federico Carbone. Writing—original draft: Federico Carbone, Maria Bertolotto. Writing—review and editing: all authors.

ACKNOWLEDGEMENTS

This study was supported by 'RCR-2022-23682288 – Rete CARDIOLOGICA- Integrated strategies for the study of tissue and molecular determinants of vulnerable atherosclerotic plaque – Procedura nota DGRIC n. 1401 del 13/04/2022 Fondo progetti reti EF 2022'. Work was also supported by #NEXTGENERATIONEU (NGEU) and funded by the Ministry of University and Research (MUR), National Recovery and Resilience Plan (NRRP), project MNESYS (PE0000006) – (DN. 1553 11.10.2022). Graphical Abstract was created in BioRender. Montecucco, F. (2025) https://BioRender.com/tuih2nw.

CONFLICT OF INTEREST STATEMENT

None to be declared.

DATA AVAILABILITY STATEMENT

Individual-level clinical data and bronchoalveolar lavage (BAL) datasets underlying the findings of this study were collected under Regional Ethics Committee approval ILDFIBRO020; CER Liguria 523/2020 and contain potentially identifying health information; therefore, they are not publicly available. De-identified data (including BAL MMP-9, TIMP-1 and derived MMP-9/TIMP-1 ratios), along with analysis scripts used for the statistical models reported in the manuscript, will be made available from the corresponding author upon reasonable request and subject to approval by the Ethics Committee and execution of appropriate data-sharing agreements. Raw and processed outputs from the experimental assays performed in this study (ELISA readouts, zymography gels and densitometry and immunofluorescence images) are available from the corresponding author upon reasonable request. The single-cell RNA-seq datasets reanalyzed in this work are publicly available from GEO under accessions GSE136831 (Kaminski/Rosas) and GSE135893 (Banovich/Kropski). These external resources were used as described in the Sections 2 and 3 of the manuscript.

ORCID

Emanuela Barisione https://orcid.org/0000-0001-5365-134X
Fabrizio Montecucco https://orcid.org/0000-0003-0823-8729
Federico Carbone https://orcid.org/0000-0003-2957-4078

REFERENCES

1. Althobiani MA, Russell AM, Jacob J, et al. Interstitial lung disease: a review of classification, etiology, epidemiology, clinical diagnosis, pharmacological and non-pharmacological treatment. *Front Med (Lausanne)*. 2024;11:1296890.
2. Kolb M, Vasakova M. The natural history of progressive fibrosing interstitial lung diseases. *Respir Res*. 2019;20(1):57.
3. Greenlee KJ, Werb Z, Kheradmand F. Matrix metalloproteinases in lung: multiple, multifarious, and multifaceted. *Physiol Rev*. 2007;87(1):69-98.
4. Shimada A, Koga T, Oshita Y, Hanada M, Nagafuchi Y, Aizawa H. Reduced pulmonary function is associated with enhanced inflammation and tissue inhibitor of metalloproteinase 1 concentration in the bronchoalveolar lavage fluid of patients with lung parenchymal sarcoidosis. *Kurume Med J*. 2008;55(1–2):13-17.
5. Radomska-Lesniewska DM, Skopinska-Rozewska E, Jankowska-Steifer E, et al. N-acetylcysteine inhibits IL-8 and MMP-9 release and ICAM-1 expression by bronchoalveolar cells from interstitial lung disease patients. *Pharmacol Rep*. 2010;62(1):131-138.
6. Amubieya O, Todd JL, Neely ML, et al. Associations of circulating matrix metalloproteinases and tissue inhibitors of matrix metalloproteinases with clinically relevant outcomes in idiopathic pulmonary fibrosis: data from the IPF-PRO registry. *PLoS One*. 2024;19(10):e0312044.
7. Robert S, Gicquel T, Victoni T, et al. Involvement of matrix metalloproteinases (MMPs) and inflammasome pathway in molecular mechanisms of fibrosis. *Biosci Rep*. 2016;36(4):e00360.

8. Zuo WL, Zhao JM, Huang JX, et al. Effect of bosentan is correlated with MMP-9/TIMP-1 ratio in bleomycin-induced pulmonary fibrosis. *Biomed Rep*. 2017;6(2):201-205.
9. Charzewski L, Krzysko KA, Lesyng B. Structural characterisation of inhibitory and non-inhibitory MMP-9-TIMP-1 complexes and implications for regulatory mechanisms of MMP-9. *Sci Rep*. 2021;11(1):13376.
10. Kou M, Jiao Y, Li Z, et al. Real-world safety and effectiveness of pirfenidone and nintedanib in the treatment of idiopathic pulmonary fibrosis: a systematic review and meta-analysis. *Eur J Clin Pharmacol*. 2024;80(10):1445-1460.
11. Chong WH, Agrawal D, Tan ZY, et al. A systematic review and meta-analysis of the clinical benefits and adverse reactions of anti-fibrotics in non-IPF progressive fibrosing ILD. *Heart Lung*. 2024;68:242-253.
12. Richeldi L, du Bois RM, Raghu G, et al. Efficacy and safety of nintedanib in idiopathic pulmonary fibrosis. *N Engl J Med*. 2014;370(22):2071-2082.
13. Distler O, Highland KB, Gahlemann M, et al. Nintedanib for systemic sclerosis-associated interstitial lung disease. *N Engl J Med*. 2019;380(26):2518-2528.
14. Ikeda S, Ogura T, Kato T, et al. Nintedanib plus chemotherapy for small cell lung cancer with comorbid idiopathic pulmonary fibrosis. *Ann Am Thorac Soc*. 2024;21(4):635-643.
15. Makiguchi T, Tanaka H, Okudera K, Taima K, Tasaka S. Safety and feasibility of carboplatin and paclitaxel in combination with nintedanib for non-small cell lung cancer patients with idiopathic pulmonary fibrosis: a prospective pilot study. *Transl Lung Cancer Res*. 2023;12(4):719-726.
16. Raghu G, Remy-Jardin M, Richeldi L, et al. Idiopathic pulmonary fibrosis (an update) and progressive pulmonary fibrosis in adults: an official ATS/ERS/JRS/ALAT clinical practice guideline. *Am J Respir Crit Care Med*. 2022;205(9):e18-e47.
17. Barisione E, Salio M, Romagnoli M, Pratico A, Bargagli E, Corbetta L. Competence in transbronchial cryobiopsy. *Panminerva Med*. 2019;61(3):290-297.
18. Graham BL, Steenbruggen I, Miller MR, et al. Standardization of spirometry 2019 update. An official American Thoracic Society and European Respiratory Society technical Statement. *Am J Respir Crit Care Med*. 2019;200(8):e70-e88.
19. du Bois RM. Fibroblastic foci: time to be counted? *Chest*. 2006;130(1):3-5.
20. Herrera JA, Dingle L, Montero MA, et al. The UIP/IPF fibroblastic focus is a collagen biosynthesis factory embedded in a distinct extracellular matrix. *JCI Insight*. 2022;7(16):e156115.
21. Giannoni P, Grosso M, Fugazza G, et al. Establishment and characterization of a novel fibroblastic cell line (SCI13D) derived from the Broncho-alveolar lavage of a patient with fibrotic hypersensitivity pneumonitis. *Biomedicine*. 2021;9(9):1193.
22. Dolivo DM, Larson SA, Dominko T. FGF2-mediated attenuation of myofibroblast activation is modulated by distinct MAPK signaling pathways in human dermal fibroblasts. *J Dermatol Sci*. 2017;88(3):339-348.
23. Giannoni P, Barisione E, Grosso M, et al. Bronchoalveolar lavage derived fibroblasts from interstitial lung disease patients: a chance to exploit 2D/3D model of pulmonary fibrosis in vitro. *Front Biosci (Landmark ed)*. 2025;30(7):38726.
24. Ministrini S, Andreozzi F, Montecucco F, et al. Neutrophil degranulation biomarkers characterize restrictive echocardiographic pattern with diastolic dysfunction in patients with diabetes. *Eur J Clin Investig*. 2021;51(12):e13640.
25. Di Ciaula A, Liberale L, Portincasa P, et al. Neutrophil degranulation, endothelial and metabolic dysfunction in unvaccinated long COVID patients. *Eur J Clin Investig*. 2024;54(4):e14155.
26. Montecucco F, Di Marzo V, da Silva RF, et al. The activation of the cannabinoid receptor type 2 reduces neutrophilic protease-mediated vulnerability in atherosclerotic plaques. *Eur Heart J*. 2012;33(7):846-856.
27. Bertolotto M, Contini P, Ottonello L, Pende A, Dallegri F, Montecucco F. Neutrophil migration towards C5a and CXCL8 is prevented by non-steroidal anti-inflammatory drugs via inhibition of different pathways. *Br J Pharmacol*. 2014;171(14):3376-3393.
28. Russo E, Bertolotto M, Zanetti V, et al. Role of uric acid in vascular remodeling: cytoskeleton changes and migration in VSMCs. *Int J Mol Sci*. 2023;24(3):2960.
29. Adams TS, Schupp JC, Poli S, et al. Single-cell RNA-seq reveals ectopic and aberrant lung-resident cell populations in idiopathic pulmonary fibrosis. *Sci Adv*. 2020;6(28):eaba1983.
30. Habermann AC, Gutierrez AJ, Bui LT, et al. Single-cell RNA sequencing reveals profibrotic roles of distinct epithelial and mesenchymal lineages in pulmonary fibrosis. *Sci Adv*. 2020;6(28):eaba1972.
31. Hao Y, Stuart T, Kowalski MH, et al. Dictionary learning for integrative, multimodal and scalable single-cell analysis. *Nat Biotechnol*. 2024;42(2):293-304.
32. Hao Y, Hao S, Andersen-Nissen E, et al. Integrated analysis of multimodal single-cell data. *Cell*. 2021;184(13):3573-3587.e29.
33. Stuart T, Butler A, Hoffman P, et al. Comprehensive integration of single-cell data. *Cell*. 2019;177(7):1888-1902.e21.
34. Butler A, Hoffman P, Smibert P, Papalexi E, Satija R. Integrating single-cell transcriptomic data across different conditions, technologies, and species. *Nat Biotechnol*. 2018;36(5):411-420.
35. Satija R, Farrell JA, Gennert D, Schier AF, Regev A. Spatial reconstruction of single-cell gene expression data. *Nat Biotechnol*. 2015;33(5):495-502.
36. Love MI, Huber W, Anders S. Moderated estimation of fold change and dispersion for RNA-seq data with DESeq2. *Genome Biol*. 2014;15(12):550.
37. Sindhu A, Jadhav U, Ghewade B, Wagh P, Yadav P. Unveiling the diagnostic potential: a comprehensive review of bronchoalveolar lavage in interstitial lung disease. *Cureus*. 2024;16(1):e52793.
38. Meyer KC, Raghu G. Bronchoalveolar lavage for the evaluation of interstitial lung disease: is it clinically useful? *Eur Respir J*. 2011;38(4):761-769.
39. Meyer KC, Raghu G, Baughman RP, et al. An official American Thoracic Society clinical practice guideline: the clinical utility of bronchoalveolar lavage cellular analysis in interstitial lung disease. *Am J Respir Crit Care Med*. 2012;185(9):1004-1014.
40. Tzilas V, Digalaki A, Bouros E, Avdoula E, Tzouvelekis A, Bouros D. Diagnostic utility of bronchoalveolar lavage lymphocytosis in patients with interstitial lung diseases. *Respiration*. 2023;102(11):944-947.
41. Zhang S, Boers LS, de Brabander J, et al. The alveolar fibroproliferative response in moderate to severe COVID-19-related acute respiratory distress syndrome and 1-yr follow-up. *Am J Physiol Lung Cell Mol Physiol*. 2024;326(1):L7-L18.
42. Midulla F, Strappini P, Sandstrom T, et al. Cellular and non-cellular components of bronchoalveolar lavage fluid in HIV-1-infected children with radiological evidence of interstitial lung damage. *Pediatr Pulmonol*. 2001;31(3):205-213.

43. Van Hoecke L, Job ER, Saelens X, Roose K. Bronchoalveolar lavage of murine lungs to analyze inflammatory cell infiltration. *J Vis Exp*. 2017;123:55398.
44. Yu G, Kovkarova-Naumovski E, Jara P, et al. Matrix metalloproteinase-19 is a key regulator of lung fibrosis in mice and humans. *Am J Respir Crit Care Med*. 2012;186(8):752-762.
45. Bormann T, Maus R, Stolper J, et al. Role of matrix metalloprotease-2 and MMP-9 in experimental lung fibrosis in mice. *Respir Res*. 2022;23(1):180.
46. Ruiz V, Ordonez RM, Berumen J, et al. Unbalanced collagenases/TIMP-1 expression and epithelial apoptosis in experimental lung fibrosis. *Am J Physiol Lung Cell Mol Physiol*. 2003;285(5):L1026-L1036.
47. Madtes DK, Elston AL, Kaback LA, Clark JG. Selective induction of tissue inhibitor of metalloproteinase-1 in bleomycin-induced pulmonary fibrosis. *Am J Respir Cell Mol Biol*. 2001;24(5):599-607.
48. Kim KH, Burkhart K, Chen P, et al. Tissue inhibitor of metalloproteinase-1 deficiency amplifies acute lung injury in bleomycin-exposed mice. *Am J Respir Cell Mol Biol*. 2005;33(3):271-279.
49. Chen P, Farivar AS, Mulligan MS, Madtes DK. Tissue inhibitor of metalloproteinase-1 deficiency abrogates obliterative airway disease after heterotopic tracheal transplantation. *Am J Respir Cell Mol Biol*. 2006;34(4):464-472.
50. Dong J, Ma Q. TIMP1 promotes multi-walled carbon nanotube-induced lung fibrosis by stimulating fibroblast activation and proliferation. *Nanotoxicology*. 2017;11(1):41-51.
51. Wu L, Luo Z, Zheng J, et al. IL-33 can promote the process of pulmonary fibrosis by inducing the imbalance between MMP-9 and TIMP-1. *Inflammation*. 2018;41(3):878-885.
52. Yu SH, Liu LJ, Lv B, et al. Inhibition of bleomycin-induced pulmonary fibrosis by bone marrow-derived mesenchymal stem cells might be mediated by decreasing MMP9, TIMP-1, INF-gamma and TGF-beta. *Cell Biochem Funct*. 2015;33(6):356-366.
53. Chakraborty A, Wang C, Hodgson-Garms M, et al. Induced pluripotent stem cell-derived mesenchymal stem cells reverse bleomycin-induced pulmonary fibrosis and related lung stiffness. *Biomed Pharmacother*. 2024;178:117259.
54. Duch P, Diaz-Valdivia N, Ikemori R, et al. Aberrant TIMP-1 overexpression in tumor-associated fibroblasts drives tumor progression through CD63 in lung adenocarcinoma. *Matrix Biol*. 2022;111:207-225.
55. Selvaraj G, Kaliamurthi S, Lin S, Gu K, Wei DQ. Prognostic impact of tissue inhibitor of Metalloproteinase-1 in non- small cell lung cancer: systematic review and meta-analysis. *Curr Med Chem*. 2019;26(42):7694-7713.
56. Grunwald B, Schoeps B, Kruger A. Recognizing the molecular multifunctionality and interactome of TIMP-1. *Trends Cell Biol*. 2019;29(1):6-19.

SUPPORTING INFORMATION

Additional supporting information can be found online in the Supporting Information section at the end of this article.

How to cite this article: Bertolotto M, de Totero D, Giannoni P, et al. Fibroblast-driven MMP-9/TIMP-1 imbalance in bronchoalveolar lavage reflects fibrotic progression in interstitial lung disease. *Eur J Clin Invest*. 2025;00:e70162. doi:10.1111/eci.70162